

Electronic Supporting Information (ESI)

# RAFT Polymerization and Associated Reactivity Ratios of Methacrylate- Functionalized Mixed Bio-oil Constituents

Angela L. Holmberg,<sup>a</sup> Michael G. Karavolias,<sup>a</sup> and Thomas H. Epps, III<sup>\*a,b</sup>

<sup>a</sup>*Department of Chemical and Biomolecular Engineering, University of Delaware, Newark, Delaware 19716, USA. \*E-mail: thepps@udel.edu*

<sup>b</sup>*Department of Materials Science and Engineering, University of Delaware, Newark, Delaware 19716, USA.*

## Nomenclature and color key applied throughout the manuscript and ESI

The acronyms for the monomers and corresponding polymers (in parentheses) are listed below. For example, guaiacol methacrylate is denoted as GM, and poly(guaiacol methacrylate) is denoted as PGM. Color codes are listed to the right of each constituent.

### Constituents of bio-oil methacrylate-1 (BOM-1, PBOM-1)

1. Guaiacol methacrylate (GM, PGM)..... light blue
2. Creosol methacrylate (CM, PCM) ..... purple
3. 4-Ethylguaiacol methacrylate (EM, PEM).....pink
4. Vanillin methacrylate (VM, PVM) .....green

### Constituents of bio-oil methacrylate-2 (BOM-2, PBOM-2)

1. Vanillin methacrylate (VM, PVM) .....green
2. Phenyl methacrylate (PM, PPM) .....red
3. *n*-Butyl methacrylate (BM, PBM) .....dark blue
4. Lauryl methacrylate (LM, PLM) ..... orange

### Miscellaneous acronyms

1. Nuclear magnetic resonance (NMR)
2. Advanced Chemistry Development, Inc. (ACD)
3. N,N'-Dimethylformamide (DMF)
4. Tetrahydrofuran (THF)
5. Tetramethylsilane (TMS)
6. Size-exclusion chromatography (SEC)

## Interpretation of $^1\text{H}$ NMR spectra from samples with mixed monomers

Monomer and polymer compositions for each sample were quantified using the characteristic  $^1\text{H}$  NMR peaks indicated below, after conversion was confirmed to be between 6 mol% and 20 mol%. Example  $^1\text{H}$  NMR spectra for the monomers (Fig. S1), homopolymers (Fig. S2 and S3), and bio-oil aliquots (Fig. S4) are available for reference on pages S6–S9.

### Composition of reactivity ratio samples containing GM, CM, EM, and/or VM

*VM–EM reactivity ratio samples:* Monomer compositions were determined using (i) the aldehyde proton in VM (9.96 ppm), (ii) the allyl protons in VM (6.39 ppm and 5.81 ppm), and (iii) the allyl protons in EM (6.35 ppm and 5.73 ppm). Polymer compositions were determined using (i) the aldehyde proton in PVM (PVM-1H<sub>a</sub> in Fig. S2) and (ii) two aromatic protons in PEM (PEM-2H<sub>a</sub> in Fig. S2) *via* both manual integration and peak-fitting approaches. Both manual integration and peak-fitting methods were used to improve the confidence in the polymer composition measurements. The peak-fitting approach used tools available in ACD/NMR Processor Software<sup>1</sup> and was necessary for refining the NMR measurements due to peak overlap. For examples in which peak overlap was insignificant (*i.e.*, in select reactivity ratio experiments for BOM-2), the peak-fitting tools were not used, as manual integration was sufficient.

*VM–CM reactivity ratio samples:* Monomer compositions were determined using (i) the aldehyde proton in VM (9.96 ppm), (ii) the allyl protons in VM (6.39 ppm and 5.81 ppm), and (iii) the allyl protons in CM (6.35 ppm and 5.73 ppm). Polymer compositions were determined using (i) the aldehyde in PVM (PVM-1H<sub>a</sub> in Fig. S2) and (ii) two aromatic protons in PCM (PCM-2H<sub>a</sub> in Fig. S2) *via* both manual integration and peak-fitting approaches.

*EM–CM reactivity ratio sample:* The monomer composition was determined using (i) the allyl protons in EM and CM (6.35 ppm and 5.73 ppm), (ii) the aliphatic ethyl and methyl protons in EM (2H at 2.64 ppm and 3H at 1.24 ppm), and (iii) the phenyl-substituent methyl protons in CM (3H at 2.35 ppm). The polymer composition was determined using (i) the aliphatic methyl protons in PEM (PEM-3H<sub>c</sub> in Fig. S2), (ii) select aromatic protons in PEM and PCM (PCM-2H<sub>a</sub> and PEM-2H<sub>a</sub> in Fig. S2), and (iii) the methoxy protons in PEM and PCM (PEM-3H<sub>b</sub> and PCM-3H<sub>b</sub> in Fig. S2) *via* both manual integration and peak-fitting approaches.

*EM–GM reactivity ratio sample:* The monomer composition was determined using (i) the allyl protons in EM (6.35 ppm and 5.73 ppm) and (ii) the allyl protons in GM (6.36 ppm and 5.74 ppm). The polymer composition was determined using (i) two aromatic protons in PEM (PEM-2H<sub>a</sub> in Fig. S2) and (ii) two aromatic protons in PGM (PGM-2H<sub>a</sub> in Fig. S2) *via* both manual integration and peak-fitting approaches.

Instead of collecting reactivity ratio data for VM–GM and CM–GM, the reactivity ratios were assumed to equal one, the approximate value that was measured for all of the above monomer pairs.

### Composition of reactivity ratio samples containing VM, PM, BM, and/or LM

*VM–PM reactivity ratio samples:* Monomer compositions were determined using (i) the aldehyde proton in VM (9.96 ppm), (ii) the allyl protons in VM (6.39 ppm and 5.81 ppm), (iii) the methoxy protons in VM (3H at 3.90 ppm), and (iv) the allyl protons in PM (6.35 ppm and 5.75 ppm). Characteristic polymer peaks for PVM and PPM overlapped even after drying, so polymer compositions were determined using the

change in the peak area for the aldehyde proton in VM (9.96 ppm), the allyl protons in VM (6.39 ppm and 5.81 ppm), and the allyl protons in PM (6.35 ppm and 5.75 pm) between the aliquots taken before and after polymerization. These spectra were normalized to (i) DMF protons or (ii) the aldehyde protons in VM and PVM. For example, if the peaks representing allyl protons in VM and PM all lost one unit of area according to spectra normalized to DMF, then the composition of the product polymer would be 0.5 mole-fraction VM ( $F_{VM} = 0.5$ ). This approach gains accuracy with increasing conversion, so restricting samples to conversions >6 mol% was necessary for reducing scatter in the data.

*VM–BM reactivity ratio samples:* Monomer compositions were determined using (i) the aldehyde proton in VM (9.96 ppm), (ii) the allyl protons in VM (6.39 ppm and 5.81 ppm), (iii) the allyl protons in BM (6.10 ppm and 5.54 ppm), and (iv) the aliphatic methyl protons in BM (3H at 0.95 ppm). Polymer compositions were determined using (i) the aldehyde proton in PVM (PVM-1H<sub>a</sub> in Fig. S3), (ii) all methyl protons in PBM (PBM-3H<sub>b</sub> and PBM-3H<sub>c</sub> in Fig. S3), and (iii) the methoxy protons in PBM (PBM-2H<sub>a</sub> in Fig. S3) *via* both aliquots and dried samples as well as both manual integration and peak-fitting approaches.

*VM–LM reactivity ratio samples:* Monomer compositions were determined using (i) the aldehyde proton in VM (9.96 ppm), (ii) the allyl protons in VM (6.39 ppm and 5.81 ppm), (iii) the allyl protons in LM (6.10 ppm and 5.54 ppm), (iv) the methoxy protons in LM (2H at 4.14 ppm), and (v) the aliphatic methyl protons in LM (3H at 0.88 ppm). Polymer compositions were determined using the change in the peak area for (i) the allyl protons in VM (6.39 ppm and 5.81 ppm), (ii) the allyl protons in LM (6.10 ppm and 5.54 ppm), and (iii) the methoxy protons in LM (2H at 4.14 ppm) between aliquots taken before and after polymerization. These spectra were normalized to the aldehyde protons in VM and PVM.

*BM–LM reactivity ratio samples:* Monomer compositions were determined using (i) the aliphatic methyl protons in BM (3H at 0.95 ppm) and (ii) the aliphatic methyl protons in LM (3H at 0.88 ppm). Polymer compositions were determined using (i) the aliphatic methyl protons in PBM (PBM-3H<sub>b</sub> in Fig. S3) and (ii) the methoxy protons in PBM and PLM (PBM-2H<sub>a</sub> and PLM-2H<sub>a</sub> in Fig. S3) *via* dried samples.

*BM–PM reactivity ratio samples:* Monomer compositions were determined using (i) the allyl protons in BM (6.10 ppm and 5.54 ppm), (ii) the methoxy protons in BM (2H at 4.15 ppm), (iii) the aliphatic methyl protons in BM (3H at 0.95 ppm), and (iv) the allyl protons in PM (6.35 ppm and 5.75 pm). Polymer compositions were determined using (i) all methyl protons in PBM (PBM-3H<sub>b</sub> and PBM-3H<sub>c</sub> in Fig. S4), (ii) the methoxy protons in PBM (PBM-2H<sub>a</sub> in Fig. S3), and either (iii<sub>a</sub>) the aromatic protons in PPM (PPM-5H<sub>a</sub> in Fig. S3) or (iii<sub>b</sub>) the methyl protons in PPM (PPM-3H<sub>b</sub> in Fig. S3). The fraction of PPM in the sample was defined by iii<sub>a</sub> in samples with low (<0.4 mole-fraction) PM content, iii<sub>b</sub> in samples with high (>0.7 mole-fraction) PM content, or by both iii<sub>a</sub> and iii<sub>b</sub> in samples with intermediate PM content (0.4–0.7 mole-fraction). Only ‘dried’ samples were used, and the choice of peak iii<sub>a</sub> *vs.* iii<sub>b</sub> came about due to the relative resolution of the peaks. PM was difficult to remove from samples with high (>0.7 mole-fraction) PM contents *via* normal drying processes and therefore convoluted peak iii<sub>a</sub>, whereas the accuracy of the iii<sub>b</sub> region decreased with increasing PBM content due to peak overlap.

*LM–PM reactivity ratio samples:* Monomer compositions were determined using the same procedures and restrictions as described for BM–PM, noting that two characteristic monomer peaks in LM are slightly different from those in BM (LM has 2 methoxy protons at 4.14 ppm and 3 aliphatic methyl protons at 0.88 ppm).

### **Composition of BOM-1 and PBOM-1:**

Monomer compositions in the feed of BOM-1 were determined both gravimetrically and by <sup>1</sup>H NMR analysis. In the NMR spectrum, the allyl protons (VM: 6.39 ppm, 5.81 ppm; GM: 6.36 ppm, 5.74 ppm; and EM + CM: 6.35 ppm, 5.73 ppm) and the methyl protons from the ethyl group in EM (3H at 1.24 ppm) allowed the relative fractions of VM, GM, EM, and CM to be quantified.

The compositions of dried samples of PBOM-1 were determined using the aldehyde in PVM (PVM-1H<sub>a</sub> in Fig. S3), the aromatic protons in PGM (PGM-2H<sub>a</sub> in Fig. S3), the combined aromatic protons in both PCM and PEM (PCM-2H<sub>a</sub> and PEM-2H<sub>a</sub> in Fig. S3), and the aliphatic methyl protons in PEM (PEM-3H<sub>c</sub> in Fig. S3). The reaction aliquots gave a secondary estimate of polymer composition *via* the change in area of the VM, GM, and combined EM/CM allyl peaks in reference to the aliquot extracted immediately prior to polymerization normalized in area to (i) the DMF peaks or (ii) the combined VM/PVM peak. Due to significant peak overlap, the aliquots were not used to define individual fractions of EM and CM units in the polymer; consequently, more error is reported for the EM and CM compositions than for the GM and VM compositions in PBOM-1. An example aliquot can be viewed in Fig. S5.

### **Composition of BOM-2 and PBOM-2**

The composition of monomer in the feed of BOM-2 was determined both gravimetrically and by <sup>1</sup>H NMR analysis. In the NMR spectrum, the allyl protons (VM: 6.39 ppm, 5.81 ppm; PM: 6.35 ppm, 5.75 ppm; and LM + BM: 6.10 ppm, 5.54 ppm) and the aliphatic methyl protons (BM: 0.95 ppm, LM: 0.88 ppm) allowed the relative fractions of VM, PM, LM, and BM to be quantified.

The composition of PBOM-2 as a function of conversion was determined entirely by referencing the change in area of the VM, PM, and combined LM/BM allyl peaks in reference to the aliquot extracted immediately prior to polymerization normalized in area to (i) the DMF peaks or (ii) the combined VM/PVM peak. This approach resulted in more error at low conversions (<20 mol%) due to the smaller change in allyl peak area. An example aliquot is shown in Fig. S5. Peaks in spectra from dried polymers overlapped considerably, so compositional data from the dried samples were not used.

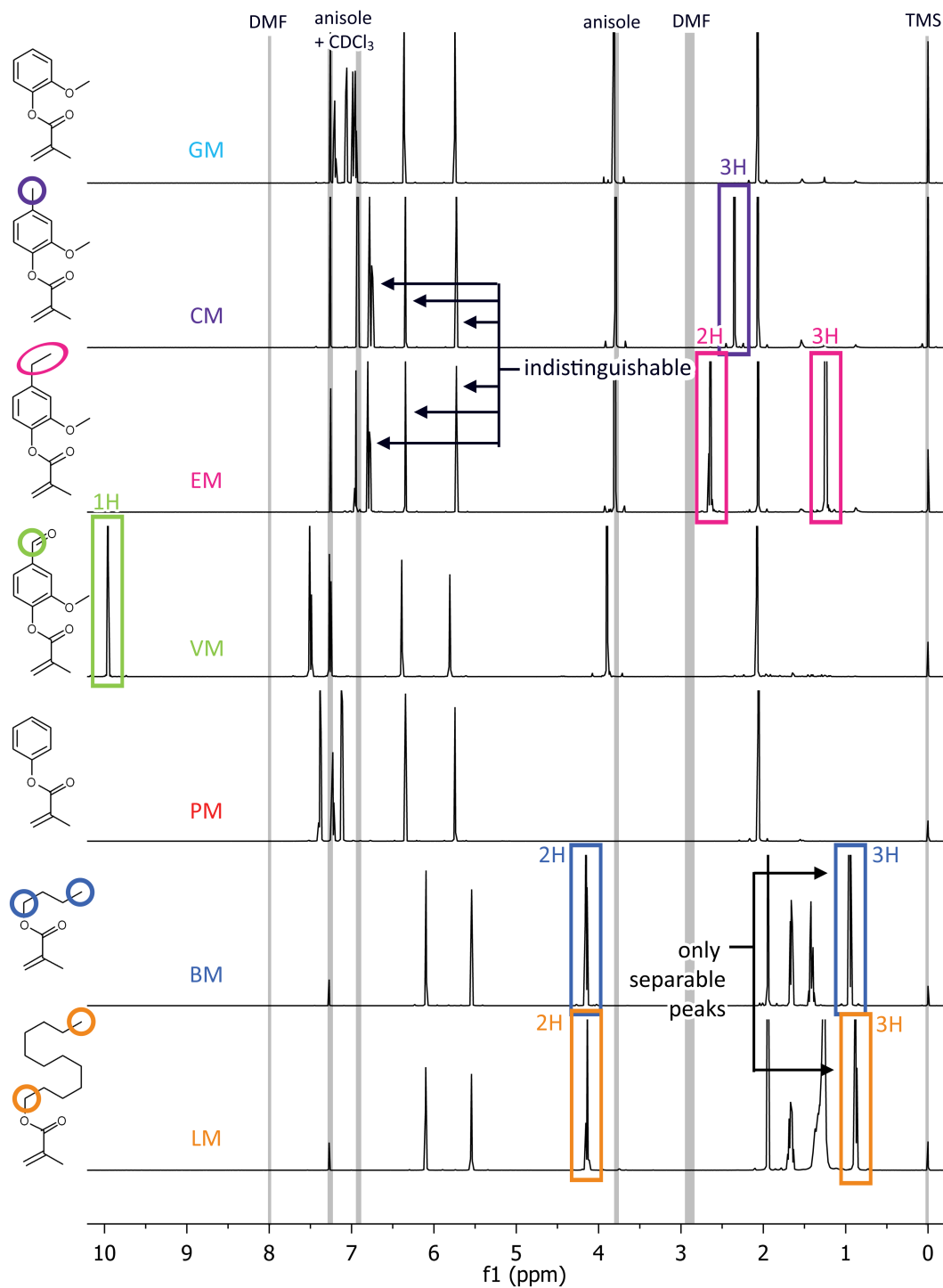


**Figure S1.**  $^1\text{H}$  NMR spectra of the monomers GM, CM, EM, VM, PM, BM, and LM. Vertical gray regions denote peak locations of solvents, and boxes indicate regions used to quantify monomer compositions in mixtures prior to polymerization. For emphasis, select peaks with identical chemical shifts (ppm) are labeled as indistinguishable. The colors refer to a specific monomer and are applied throughout the manuscript and ESI for clarity.

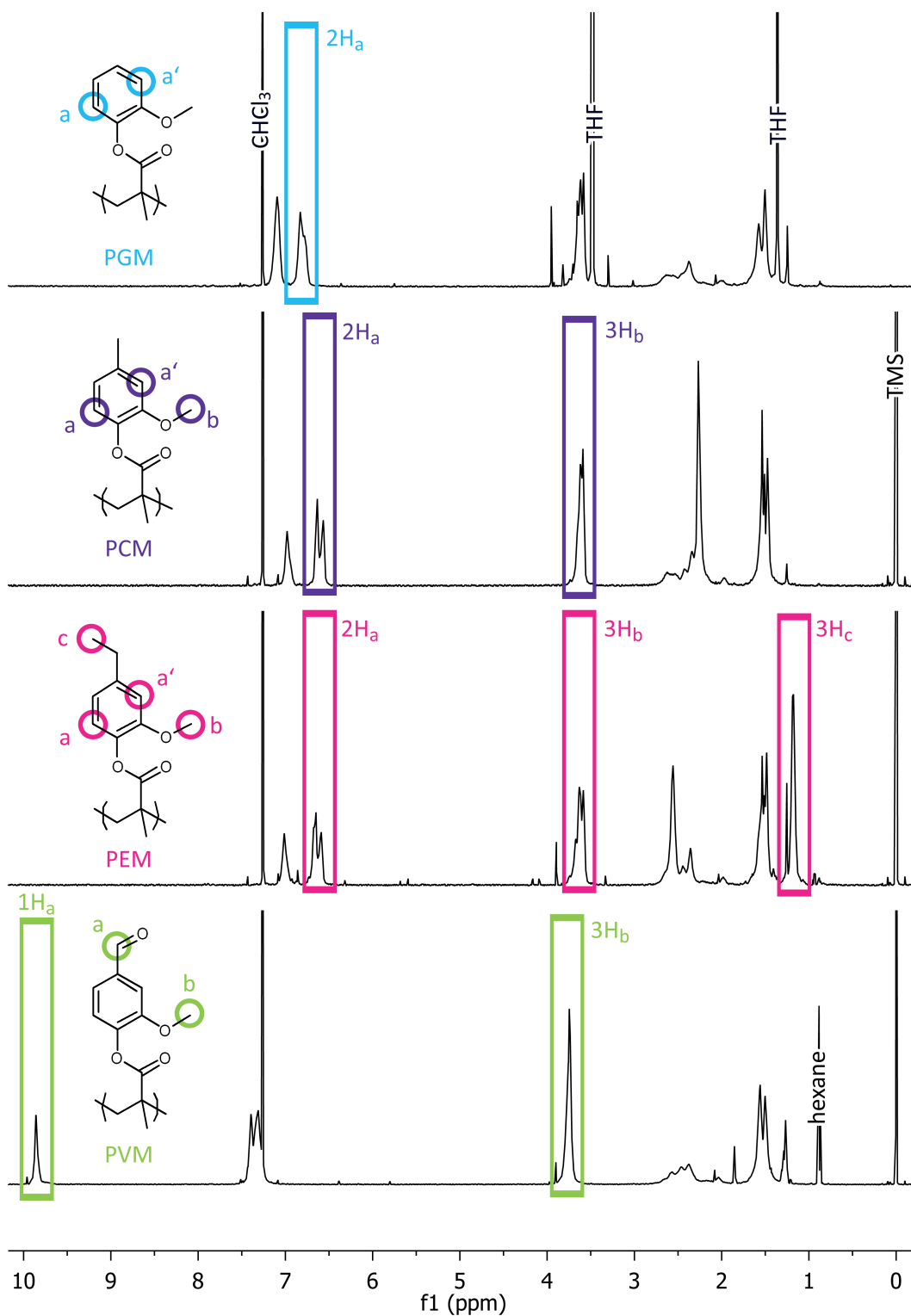


**Figure S2.**  $^1\text{H}$  NMR spectra of homopolymers synthesized from GM, CM, EM, and VM with boxes indicating regions used to quantify polymer compositions in reactivity ratio studies or in PBOM-1.

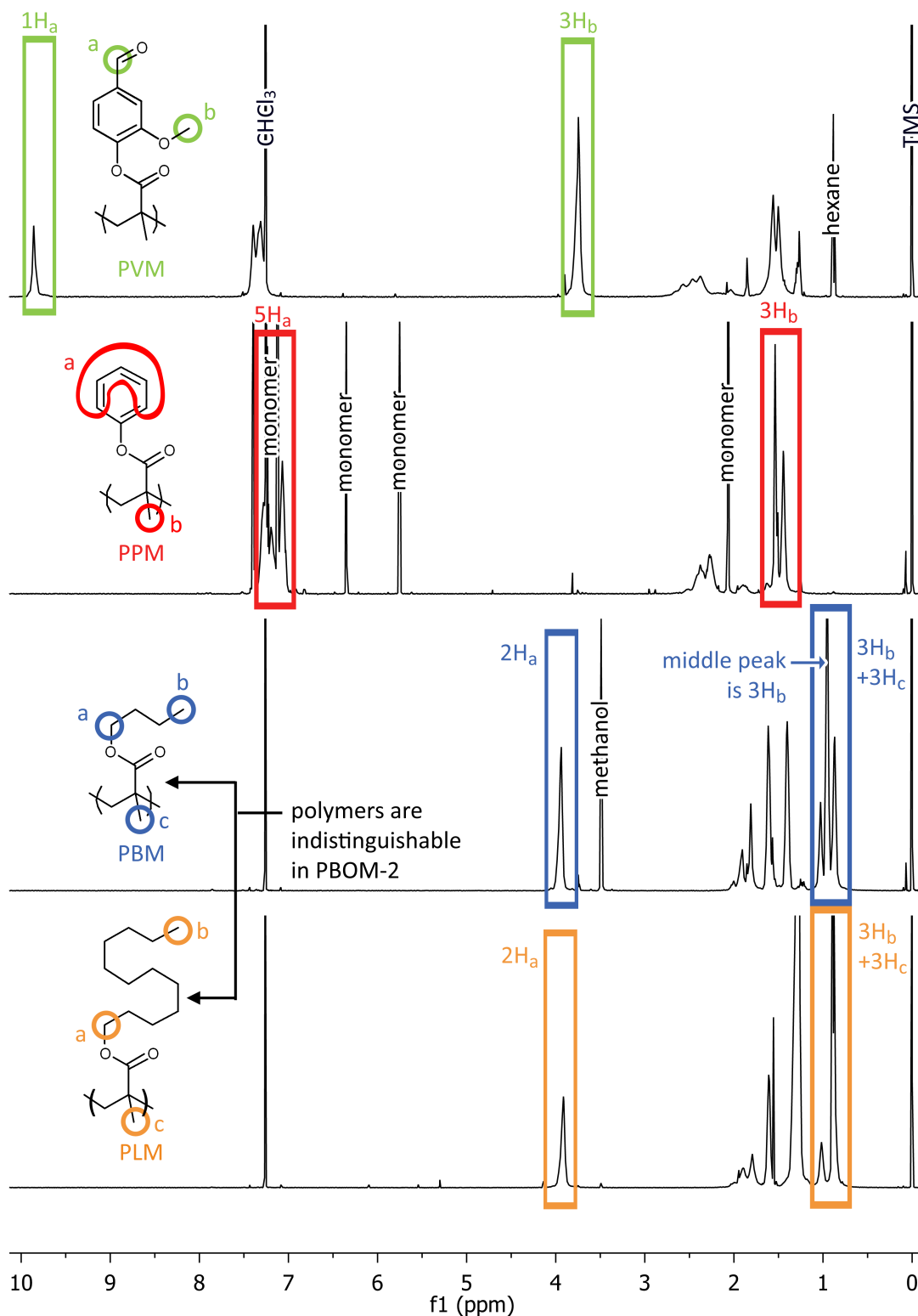


**Figure S3.**  $^1H$  NMR spectra of homopolymers synthesized from VM, PM, BM, and LM with boxes indicating regions used to quantify polymer compositions in reactivity ratio studies.

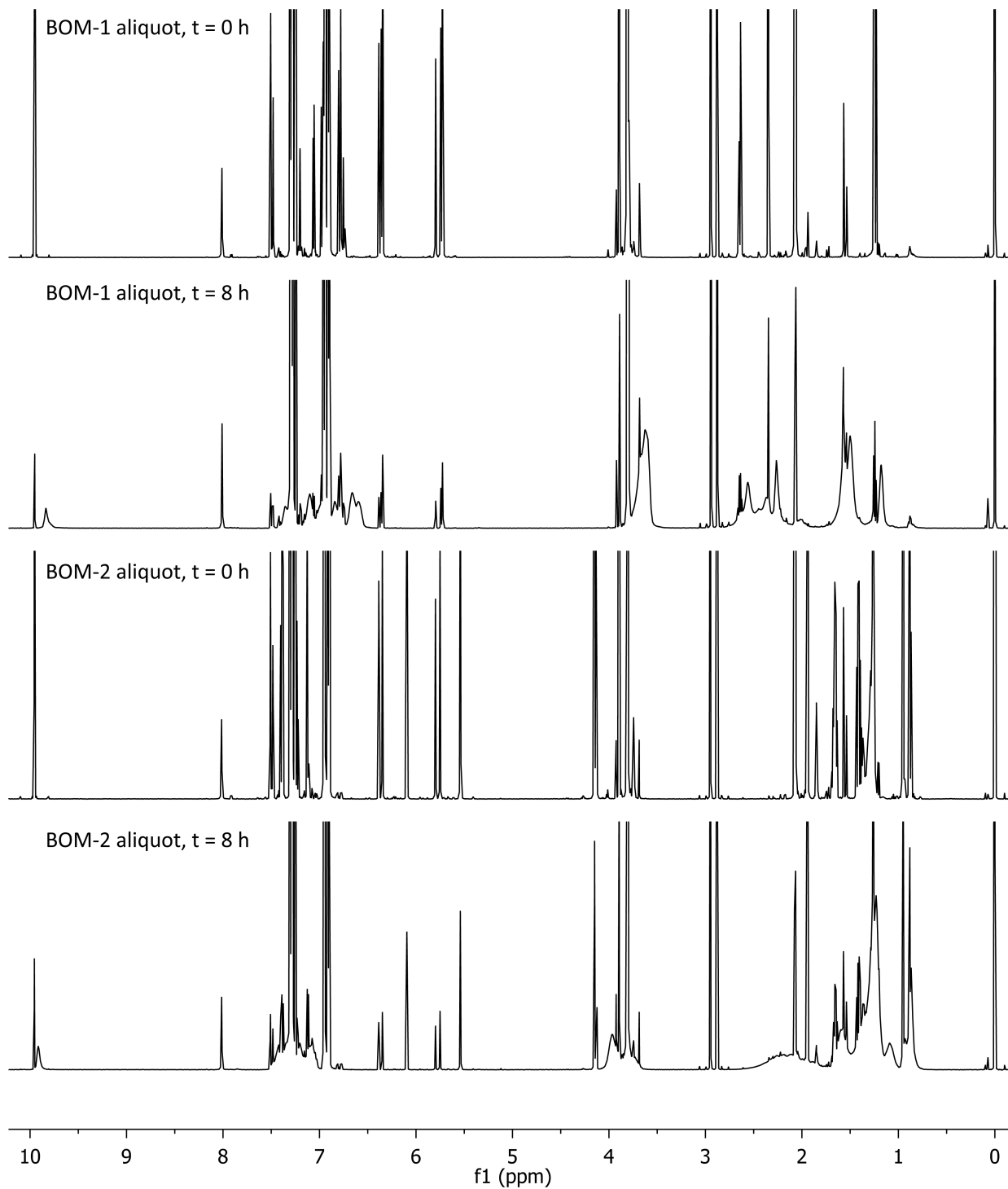


**Figure S4.** Example  $^1\text{H}$  NMR spectra of aliquots taken from the polymerizations of BOM-1 and BOM-2. The spectra are normalized by the peak area between 9.60 ppm and 10.10 ppm.

## Description of the 4<sup>th</sup> Order Runge–Kutta solver

Compositional profiles for the polymerization of four-component monomer mixtures were predicted as a function of conversion by numerically integrating the combined Walling–Briggs and Skeist equations as described by Ting *et al.*,<sup>2</sup> except for one key difference. Whereas Ting *et al.* employed Matlab's ODE45 function, we employed a classical 4<sup>th</sup> Order Runge–Kutta analysis program using equations from Chapra and Canale.<sup>3</sup> We chose to make this change because although ODE45 generally is simpler to code and solves ODEs quickly, it can fail if the equations are stiff.<sup>3</sup> The alternative we chose is more reliable than, and just as accurate as, ODE45 given the error in the composition measurements. Additionally, the computational time was reasonable (the program takes less than 3 s to solve  $j = 10,000$  steps on an average computer). The Runge–Kutta portion of the Matlab<sup>4</sup> code is as follows:

```
for i = 1:j-1
    x(i+1,1)=x(i,1)+h;
    k(1,:)=(F(i,:)-f(i,:))/(x(i,1)-1);
    fk2=f(i,')+0.5*k(1,')*h;
    Fk2=Fi(fk2,r);
    k(2,:)=(Fk2-fk2)/(x(i,1)+0.5*h-1);
    fk3=f(i,')+0.5*k(2,')*h;
    Fk3=Fi(fk3,r);
    k(3,:)=(Fk3-fk3)/(x(i,1)+0.5*h-1);
    fk4=f(i,')+k(3,')*h;
    Fk4=Fi(fk4,r);
    k(4,:)=(Fk4-fk4)/(x(i,1)+h-1);
    fa(i+1,:)=f(i,')+1/6*(k(1,')+2*k(2,')+2*k(3,')+k(4,'))*h;
    f(i+1,:)=fa(i+1,:)/sum(sum(fa(i+1,:),1),2); %%
    F(i+1,:)=Fi(f(i+1,:),r);
end
```

in which  $i$  is the sample index,  $h$  is the step size,  $j$  is the number of steps ( $1/h$ ),  $k$  and other variables containing  $k$  are predictor–corrector parameters,  $x$  is a vector of molar conversions,  $F$  is a matrix of positional polymer compositions in mole-fractions,  $f$  is a matrix of monomer compositions in mole-fractions with the feed composition in row 1,  $r$  is a matrix of reactivity ratios, and  $Fi$  is a separate function that outputs a matrix of polymer compositions after solving the Walling–Briggs equations given inputs of a monomer composition vector and a reactivity ratio matrix. The line labeled on the right by two percent signs ensures that the sum of the monomer compositions holds at unity.

## Additional information on the experimental methodology

The experimental methodology that we employed for measuring reactivity ratios ( $r_{i,j}$ ) involved greatly reduced resource consumption in comparison to conventional methods. Reactivity ratio samples usually vary only in monomer composition; the samples are diluted with solvent to confirm that changes in monomer concentration do not correspond to changes in solvent quality, a trait known to influence reactivity ratio measurements.<sup>5</sup> Other times, dilute reaction conditions are selected to enable *in situ* NMR experiments; however, these dilute reaction conditions then are extended to scaled-up multicomponent polymerizations, leading to substantial volumes of solvent waste.

In contrast, the reaction conditions that we employed were concentrated (0.94 w/w monomer/solvent) and necessary to mimic desirable near-bulk reaction conditions that reduce waste.<sup>6</sup> We also included the chain-transfer agent to reduce overall sample preparation time and confirm that reagent ratios were consistent between experiments. Specifically, we used premade samples for multiple experiments (reactivity ratio studies, kinetic studies, and other polymerizations) instead of making new mixtures of monomer, free-radical initiator, solvent, and chain-transfer agent for each experiment. The potential disadvantages of our methods were reactivity ratio samples that varied in solvent composition (the solvent was largely monomer) and polymerization times that depended on the pre-equilibrium time ( $t_{\text{init}}$ ). However, the resulting  $r_{i,j}$  were accurate enough to capture kinetic data and compositional data, so the hypothesized challenges with our methods were insignificant. The applicability of the data across all studies likely was enabled by keeping reaction conditions and concentrations consistent between samples. Hence, the reported experimental methodology is beneficial for reducing waste, saving time, and ensuring reproducibility between studies.

## Example molecular weight distributions

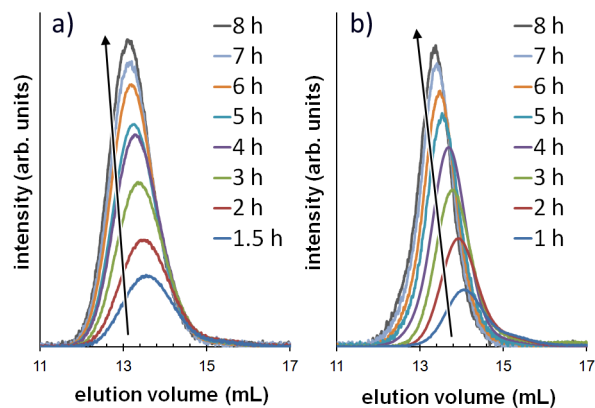


**Figure S5.** Example SEC data from the syntheses of PBOM-1 (a) and PBOM-2 (b) scaled by height to monomer conversion. Arrows indicate direction of change with respect to increasing polymerization time.

## Additional reactivity ratio data

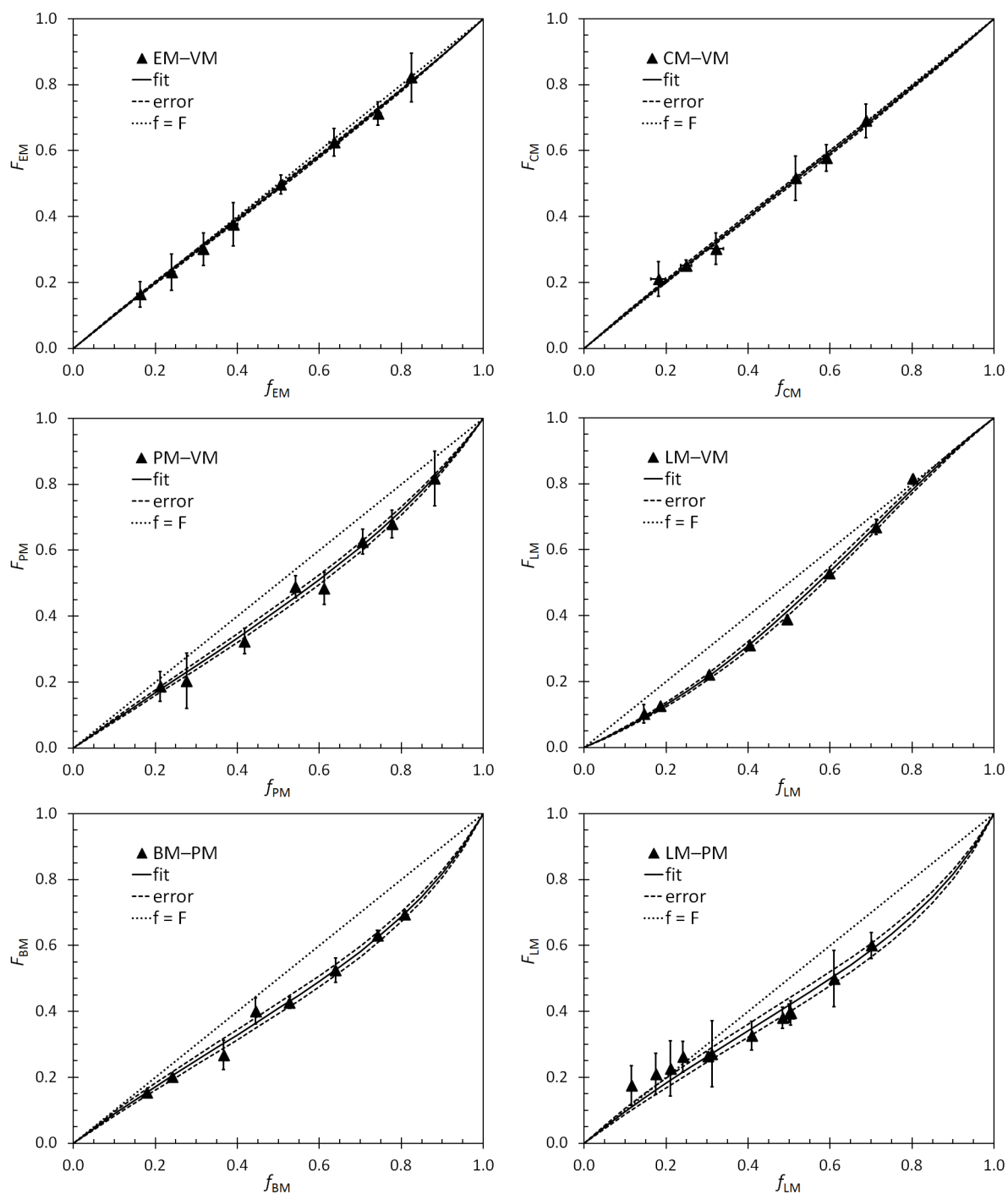


**Figure S6.** Reactivity ratio data (triangles) for all monomer pairs not illustrated in the manuscript reported with 95% confidence intervals in both  $f_i$  and  $F_i$ , Mayo–Lewis fits to the data (solid lines), and the window of mean standard error in the Mayo–Lewis fit (dashed lines). The ‘ $f = F$ ’ line (dotted) is included as a visual reference, representing  $r_{i,j} = r_{j,i} = 1$ .

## Additional compositional profile predicted for PBOM-1

Reactivity ratios ( $r_{i,j}$ ) measured for VM–EM and VM–CM spanned 0.87–0.97, and throughout the manuscript, these reactivity ratios were assumed to be nearly unity. This assumption was appropriate given the error in the measurements and the negligible change in composition with respect to conversion. Nevertheless, for reference, Fig. S7 illustrates the maximum and minimum mole-fractions of each monomer in the polymer ( $F_i$ ) as a function of molar conversion ( $x$ ) that are expected given a scenario in which all  $r_{i,j}$  in BOM-1 equal any value from 0.87–0.97.

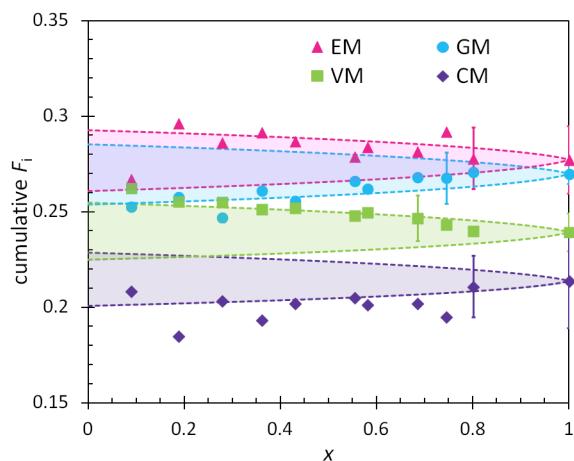


**Figure S7.** Experimentally determined composition (points) of BOM-1 as a function of monomer conversion ( $x$ , mole-fraction) overlaid with the window of possible compositions (color-coded shaded regions) given any set of  $r_{i,j}$  equal to 0.87–0.97. The majority of the error bars given at 95% confidence were removed for visual clarity, and all of the error bars overlap the theoretical composition window for a given monomer.

## References

1. ACD/NMR Processor Academic Edition: 1D NMR Processor, version 12.01, Advanced Chemistry Development, Inc.: Toronto, On, Canada, acdlabs.com, 2014.
2. J. M. Ting, T. S. Navale, F. S. Bates and T. M. Reineke, *ACS Macro Letters*, 2013, 2, 770-774.
3. S. C. Chapra and R. P. Canale, in *Numerical Methods for Engineers*, McGraw-Hill, New York, 5th edn., 1985, ch. 25.3.3, pp. 707-708.
4. MATLAB, version 8.3.0.532 (R2014a), The Mathworks, Inc.: Natick, MA, 2014.
5. M. Bercea and B. A. Wolf, *Soft Matter*, 2015, 11, 615-621.
6. M. Semsarilar and S. Perrier, *Nature Chemistry*, 2010, 2, 811-820.